Glass transitions of thin polymeric films: Speed and load dependence in lateral force microscopy

Franco Dinelli, Cynthia Buenviaje, and René M. Overney[a)]
University of Washington, Department of Chemical Engineering, Benson Hall, Box 351750, Seattle, Washington 98195

(Received 8 October 1999; accepted 26 April 2000)

The glass transition of thin polymeric films can be profitably studied using lateral force microscopy (LFM) if the system is calibrated regarding operational parameters, in particular the applied load and the scanning velocity. We have established that these two parameters significantly influence the occurrence of an apparent glass transition. In particular, we have found that the local pressure, applied by the LFM tip, is insufficient to generate a hydrostatic pressure effect causing an increase in the apparent transition temperature. In fact, at a constant scan velocity and for increased load, the apparent transition temperature decreases towards the actual bulk value. Further discussions in this article are based on viscoelastic theories. Critical time scales that are characteristic for sliding are compared to polymer relaxation times, and provide an estimate of the viscosity temperature dependence. © *2000 American Institute of Physics.* [S0021-9606(00)50428-0]

I. INTRODUCTION

An external pressure, homogeneously applied, can affect the glass transition of polymers.[1,2] It was shown that the glass transition temperature, T_g, linearly increases by increasing the external pressure (0.3 K/MPa for polystyrene).[3] This was interpreted as the effect of hampering the thermal expansion and, therefore, the formation of the free-volume necessary for the glass transition to take place. The inception of the scanning force microscope, as a contact mechanical tool to measure T_g at the polymer surface[4,5] created a powerful tool for very localized investigations of T_g. However, the pressure applied by the scanning tip in scanning force microscopy (SFM) contact experiment, typically on the order of 10^6 to 10^9 Pa, is an alleged source for significant shifts from the *actual* T_g value.

Among others, one possible SFM approach to measure surface transition values is the lateral force mode, also called lateral force microscopy (LFM). Typically, LFM relies on the measurement of the lateral force acting between tip and surface as they move one relative to the other.[6] For a closed-loop scan (i.e., forward and reverse) frictional dissipation causes a hysteresis in the lateral force. The apparent T_g value is defined as the temperature at which the frictional value[4,7,8] or the friction coefficient changes abruptly.[9] Lateral forces were also used to plastically deform the polymeric material in a very distinct manner, i.e., by forming *bundles* at elevated temperatures far above T_g.[10] Angles between the bundles and the scan direction were determined as a function of the scan frequency, and an apparent T_g value determined by the Williams–Landel–Ferry theory.[10] In all the reported LFM studies, the apparent T_g was found to significantly exceed the bulk values, sometimes up to tens of degrees.[9,10]

Very recently, another SFM mode was introduced for T_g measurements, the shear modulation mode.[5] This nonscanning SFM mode has been successfully employed to study interfacial effects on T_g values of ultrathin polystyrene films. It provided very reproducible, load independent T_g values. Strikingly, T_g values for films that exceeded a critical film thickness of about 100 nm were found to correspond well to bulk data obtained by complementary techniques, such as differential scanning calorimetry (DSC). The shear modulation method suggests that the large deviations in the apparent T_g from bulk values obtained by LFM measurements cannot be explained by a hydrostatic pressure force, but instead is caused by other operational parameters.

In this article, we will address this issue, focus our attention on the local compressibility of polymers, and discuss the apparent glass transition observed via lateral force measurements. We will consider relatively thick films (>100 nm) to avoid effects due to interaction with the substrate.[5] Hence, our conclusions are restricted to unconfined amorphous films with molecular weight higher than 20 k.

II. EXPERIMENT

Our SFM is a commercial instrument (*Explorer*, Thermomicroscopes, Inc.) where the cantilever is moved by linearized *x*, *y*, and *z* scanners. The sample holder was modified to house a cooling-heating stage manufactured by MMR Technologies Inc. The temperature can be varied in the range between 220 to 450 K with a precise control of ± 0.5 K.[5] The whole system is enclosed in a glove box that is flooded with dry nitrogen. A relative humidity value of less than 5% can be routinely achieved. This is necessary to prevent the formation of water liquid–vapor capillary necks between tip and sample.

Measurements of friction force as a function of temperature were conducted on thin films of polystyrene ($M_w = 270$ K, $M_w/M_n = 1.07$, Polymer Source, Inc.). Films of 100 nm were obtained by spin-coating polystyrene, diluted in toluene, onto H-terminated silicon wafers. Bar-shaped cantile-

a)Author to whom correspondence should be addressed.

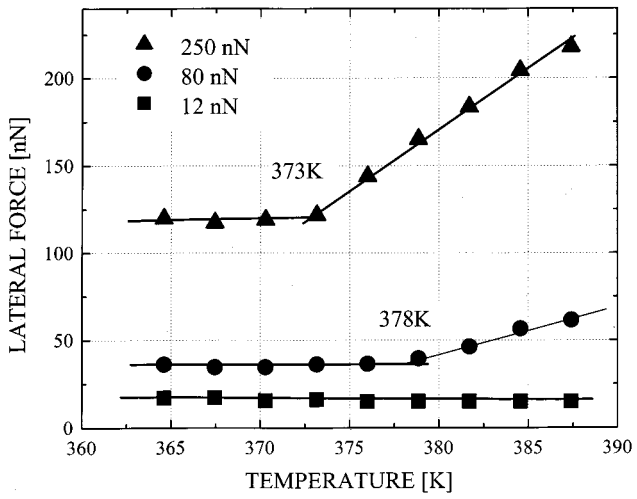

FIG. 1. Friction force versus temperature for three loads. The scan distance is 5 μm and the scan speed is 5 μm/s. At a load of 12 nN, no apparent temperature, T_C, is observed. The apparent transition temperature corresponds to T_g (373 K) if the plastic regime (bundle formation) is well initiated. In the intermediate regime, T_C (378 K) is higher than T_g.

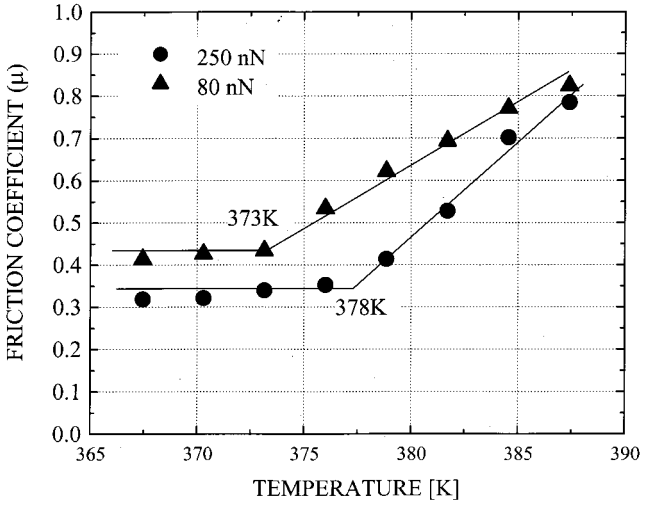

FIG. 2. Friction coefficient versus temperature for two applied loads (80 and 250 nN). As discussed in Fig. 1, T_C corresponds to T_g at a high maximum load (plastic regime). T_C is higher than T_g at a lower applied load.

vers were employed, with a normal spring constant ranging from 0.1 to 0.5 N/m. Conventionally, the friction force was obtained by the difference (divided by 2) of the average lateral force that acts on the tip when scanning a forward–backward loop (x direction). The tip was shifted (y direction) at the end of each loop to avoid work hardening and wear. The temperature was increased in increments of 2 to 3 K. A waiting time of approximately 10 min was considered sufficient to stabilize the sample temperature.

The T_g of bulk polystyrene was determined by differential scanning calorimetry (DSC) to be 373 K. Using the shear modulation mode, the T_g of the spin-coated films was found to be in good agreement with the bulk value (373±1 K).

III. RESULTS

Figure 1 shows the friction force as a function of temperature for three loads. The scan distance is 5 μm and the scan speed is 5 μm/s. It is important to mention that it was not possible to perform T_g measurements at a negative load (i.e., with the cantilever bent towards the sample), as the tip would snap off. Hence, we decided to report the applied load and not the total load, which is also comprised of the adhesive load.

At low load (12 nN), no trace of plastic deformation was noticed in the investigated area. At high load (250 nN), plastic deformation was observed in form of bundles, which were more pronounced above T_g. At an intermediate load (80 nN), no noticeable deformation was observed below T_g but became distinguishable above a critical temperature. We will name this apparent transition temperature as T_C to differentiate it from the actual glass transition temperature. From Fig. 1, it is evident that a T_C can be observed when working at high and intermediate loads. This T_C is in good agreement with T_g (373 K) at high loads (250 nN) but is higher than T_g at an intermediate load (80 nN). Strikingly, no T_C is observed at low loads (12 nN). The friction force remains constant over a wide range of temperatures even above T_g. It is important to point out that no load dependence was observed in the shear modulation mode.

Figure 2 presents the same data as in Fig. 1 in the form of temperature-dependent friction coefficients. Data is presented for two applied loads of 80 and 250 nN. At high load, T_C coincides with T_g while, at low load, T_C is larger than T_g by a few degrees.

Not only the load but also the velocity affects T_C. The interplay of scan speed and applied load on T_C and the possible initiation of plastic deformation is shown in Fig. 3. For three temperatures (378 K, 372 K, and 360 K), it is illustrated how the friction force is affected by the scan speed. A scan length of 5 μm was maintained, and only the scan speed

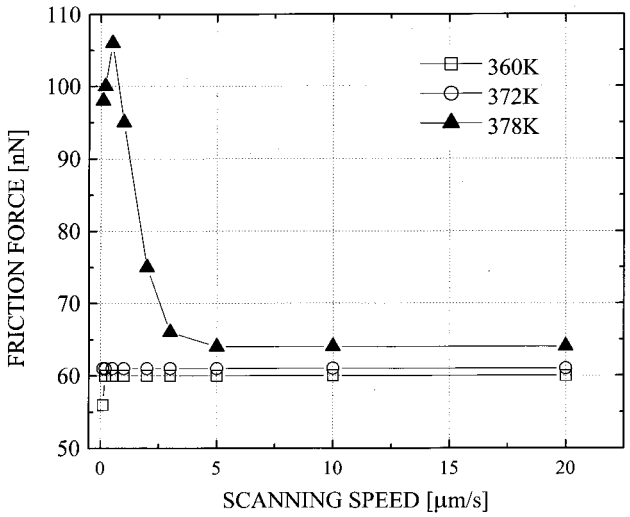

FIG. 3. Friction force versus speed at three temperatures, above and below T_g. The scan distance is 5 μm and the applied load is 15 nN. Depending on the scan speed, the friction force dramatically changes above T_g. For speeds below 3 μm/s, an increase in the friction force occurs in parallel to bundle formation in the polymer matrix.

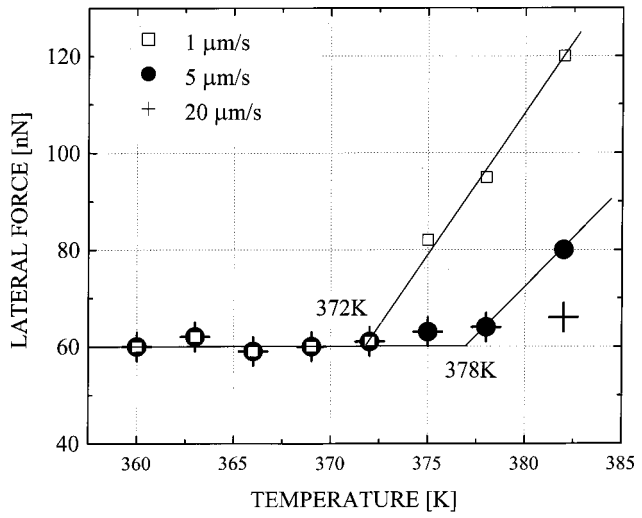

FIG. 4. Friction force versus temperature for three scan speeds. The scan distance was 5 μm and the load was 15 nN. At high speed (20 μm/s), no T_C is observed. A T_C corresponding to T_g can be observed at low speed (1 μm/s) when bundles start to appear. At intermediate scan speeds (5 μm/s), T_C is higher than T_g.

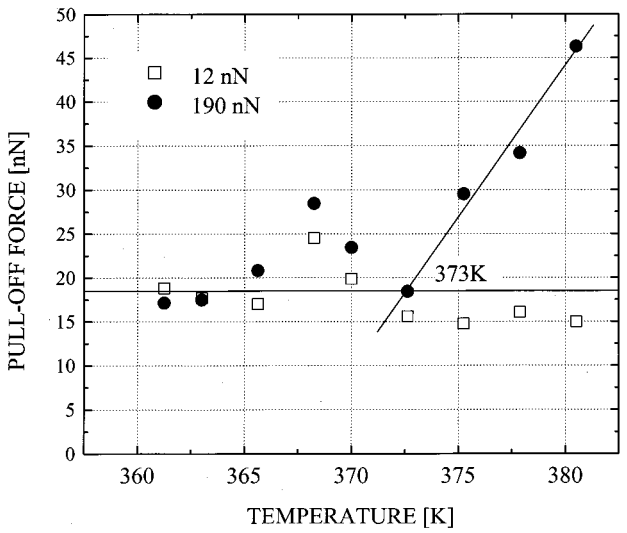

FIG. 5. Pull-off force versus temperature. Force–displacement curves were acquired at each temperature at two maximum loads (12 and 190 nN) maintaining a constant retracting speed (0.5 μm/s). Above T_g the pull-off force increases with increasing maximum load. At a maximum load of 12 nN, no T_C is observed. At a maximum load of 190 nN, T_C is equal to T_g.

was varied from 0.1 to 20 μm/s. The applied load was kept constant at 15 nN. It can be noticed that at 378 K and speeds below 3 μm/s, the friction force increased. This effect did not occur below T_g. This sudden increase in friction is well explained by the observed bundle formation.

In Fig. 4 the friction force is plotted as a function of temperature for three scan speeds. The scan distance was 5 μm and the applied load 15 nN. At high speeds (>20 μm/s), no trace of deformation nor any apparent transition was noticeable. At intermediate speeds, $T_C > T_g$ was observed. A T_C value corresponding to T_g was obtained below a critical speed ν_C, when bundles started to appear. ν_C increases with increasing load.

Measurements of the pull-off force as a function of the temperature were also carried out. In particular, the maximum applied load and the speed were varied. Below T_g, the pull-off force did not depend on these two parameters while it did above T_g. In Fig. 5, for constant retracting speed of 0.5 μm/s, it is shown that the pull-off force increased with increasing maximum load. At a load of 190 nN, pull-off force measurements clearly indicate a T_C equal to T_g. At a load of 12 nN, no T_C can be observed. Note that a decrease in velocity corresponds to an increase in contact time. In our experiments the contact time was 1 s at high maximum load and 0.1 s at low maximum load. Changing the approach speed in the range 0.01 to 0.5 μm/s confirmed our predictions. At an intermediate load of 80 nN, T_C was only equal to T_g below a critical approach speed of 0.05 μm/s.

IV. DISCUSSION

First, we will discuss the hypothesis of a shift in T_g induced by the tip-exerted pressure. We can evaluate the expected shift, ΔT, by considering a Hertzian contact. The contact radius a is given by[11]

$$a^3 = \frac{3LR(1-\nu^2)}{4E}, \tag{1}$$

where R is the tip radius, E is the sample Young's modulus, ν is the Poisson's ratio, and L is the applied load. Below T_g, with $L=15$ nN, $E=3$ GPa,[12] and $R=10$ to 50 nm, the contact radius is equal to 3 to 5 nm. Assuming that the strain induced cannot be laterally released, a hydrostatic pressure of 0.2 to 0.5 GPa results. A temperature–pressure gradient of 0.3 K/MPa (see Introduction) would therefore lead to a temperature shift (ΔT) of 60 to 150 K which is highly unrealistic. On the contrary, we found that T_C decreases with increasing applied load (Fig. 1).

This finding is not surprising as the pressure exerted by the tip is localized and limited in time. First, the tip is typically scanned over several micrometers with a scan rate of a few Hz. Assuming values of 3 to 5 nm for the contact radius, the contact area is 30 to 80 nm^2. Thus, the approximate volume affected is equivalent to a cylinder of height equal to five times the contact radius with a volume equal to 450 to 2000 nm^3.[11] In our case, the radius of gyration, R_g, is about 5 nm and the volume occupied by one molecule is $V = \frac{4}{3}\pi R_g^3 = 500$ nm^3.[13] This leaves about one to four molecules in the compression zone. Second, the contact radius is small compared to the scan length. The time of permanence over a specific area is as short as a few milliseconds per cycle. For the remaining scan cycle, the molecules are unconstrained and can relax. Additionally, one has to consider that there is always some creep and thermal drift so it is quite likely the tip never passes over the same molecules. Hence, the pressure exerted by the tip cannot be considered hydrostatic. Finally, it must be considered that the friction force is typically measured once the temperature is stabilized.[4,7–10] For isothermal scan conditions, the polymer can be considered incompressible, i.e., it undergoes mechanical deforma-

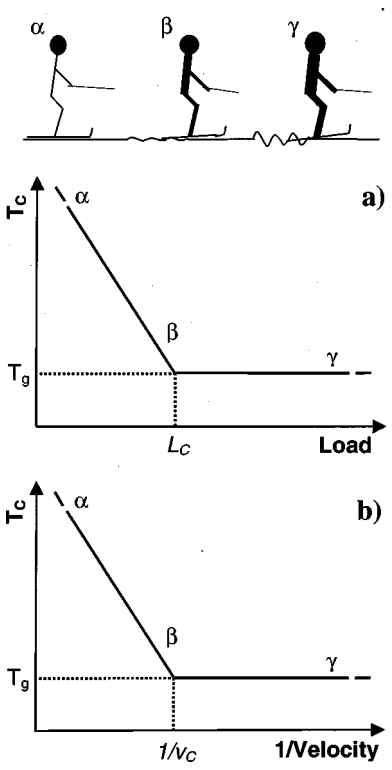

FIG. 6. Schematic representation of T_C as a function of the applied load and the scan speed. (a) Given a certain scan speed, T_C coincides with T_g at high load. By decreasing the applied load, T_C progressively increases. L_C is a critical load below which T_C starts to increase. (b) Given a certain load, T_C coincides with T_g below a critical scan speed, ν_C. By increasing the scan speed, T_C progressively increases. (α) *Water skiing*: the scan speed and the applied load are such that the tip glides over the surface below and above T_g. No transition is observed. (β) *Rippling*: the scan speed and the applied load are such that the bundle formation starts at a critical temperature, T_C is very close to T_g. (γ) *Ploughing*: the scan speed and the applied load are such that the bundle formation starts even below T_g. At T_g, the bundle depth dramatically increases.

tions but its density and free volume remain constant. This makes it even more unrealistic to expect a pressure effect on the glass transition.

As already mentioned, we observed that the apparent transition temperature increases with decreasing load, which is in contradiction to the idea of a hydrostatic pressure applied by the tip. Our findings are illustratively discussed in Fig. 6 for a water skier. At a fixed scan speed, T_C coincides with T_g at high load. By decreasing the applied load, T_C progressively increases. L_C is a critical load below which T_C starts to increase. A similar trend is found when varying the scan speed at a constant load. T_C coincides with T_g below a critical speed ν_C. By increasing the speed, T_C progressively increases. To summarize, three regimes can be defined: (α) ''ploughing'' at high load or low speed, (β) ''rippling'' for loads and speeds around L_C and ν_C, and (γ) ''water skiing'' at low load or high speed. In the following paragraphs, we will discuss the parameters responsible for the three regimes.

For a single asperity contact, the friction force can be expressed as[14]

$$F=\tau A, \tag{2}$$

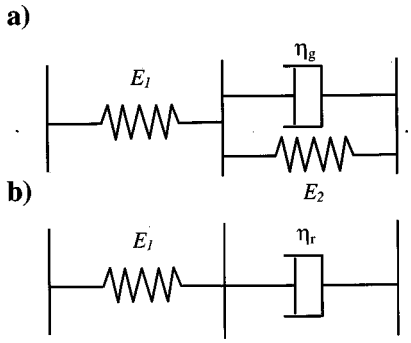

FIG. 7. Appropriate rheological models for polymer films (a) below and (b) above T_g. η_g and η_r are the viscosity constants in the glassy and rubbery states, respectively. E_1 and E_2 are two elastic constants characteristic of the material.

where A is the contact area (πa^2) and τ is the shear strength. In the ploughing regime, the applied pressure is sufficient to induce plastic deformation even below T_g, as confirmed by the appearance of bundles. At 200 nN, this is always true in the velocity range of 0.1 to 20 μm/s. In this plastic regime, according to von Misses criteria, we can write[11]

$$F=\tau\frac{L}{p_m}\cong\tau\frac{L}{1.8Y}, \tag{3}$$

where p_m is the mean pressure and Y the yield stress. Now, τ depends on the surface energy. From bulk measurements, it was already established that the surface energy of polystyrene slightly decreases at a rate of 0.05 $\mathrm{Jm^{-2}/K}$.[15] Therefore, in the temperature range explored, it is almost unvaried: at 350 K 38 $\mathrm{Jm^{-2}}$, at 390 K 36 $\mathrm{Jm^{-2}}$. This is substantiated by the fact that the pull-off force slightly decreases around T_g when the maximum load is low and the speed is high, i.e., the contact time is short (Fig. 5). In this regime, the pull-off force is mainly sensitive to surface energy variations. Thus we can assume that τ does not vary substantially. Therefore we can deduce that, in the ploughing regime, the friction force is mainly sensitive to variations of Y.

The two other regimes can be discussed by considering the viscoelastic nature of the polymer films. For a viscoelastic contact and a step loading variation, Eq. (1) can be written as[11]

$$a^3(t)=\frac{3RL_0}{8}\Phi(t), \tag{4}$$

where L_0 is the load at time zero; $\Phi(t)$ is the creep function derived by assuming an appropriate viscoelastic model. In Fig. 7, two models are introduced: the delayed elasticity model for the glassy state below T_g and the steady creep (Maxwell) model for the rubbery state above T_g. In the two cases, $a(t)$ is respectively[11]

$$a^3(t)=\frac{3RL_0}{8}\left(\frac{1}{E_1}+\frac{1}{E_2}(1-e^{-t/t_C})\right), \tag{5}$$

$$a^3(t)=\frac{3RL_0}{8}\left(\frac{1}{E_1}+\frac{1}{\eta_r}t\right), \tag{6}$$

where η_g and η_r are the viscosity constants below and above T_g, E_1 and E_2 are two elastic constants characteristic of the material, and t_C is equal to η_g/E_2. We will take $E_1=E_2=3$ GPa and assume that E_1 does not change at T_g. In the range of temperatures we explored, the main difference is represented by a large change in viscosity, as it emerges from macroscopic measurements.[12]

The time of tip permanence on the contact area t_S can be defined as

$$t_S \approx \frac{a}{\nu_S}, \tag{7}$$

where ν_S is the scan speed. Below T_g, t_C is much longer compared to the longest t_S of our experiments. This has been confirmed by the following experiment. At a temperature of 368 K, the tip was maintained in contact with the sample at various loads and times ranging from 5 to 20 min. No hole formation was observed. Therefore, we always have

$$a^3(t_S)=a_0^3=\frac{3RL_0}{8}\frac{1}{E_1}. \tag{8}$$

Above T_g, $a(t_S)$ is approximately equal to a_0 if the following condition is satisfied [from Eq. (6)]:

$$t_S \ll \frac{\eta_r}{E_1}. \tag{9}$$

In the low load regime (Fig. 1), data points were collected with ν_S equal to 5 μm/s and a_0 of roughly 3 to 5 nm [Eq. (1)]. Thereupon t_S is equal to 0.6 to 1 ms. The tip glides over the surface like a skier on water as exemplified in Fig. 6 and Eq. (9) holds at nearly all temperatures. Though almost imperceptible, a small increase occurs at 384 K. This is imputable to an increase of contact area, as τ does not change [Eq. (2)]. Therefore $a(t_S)$ must be higher than a_0. $a(t_S)$ becomes higher than a_0 if η_r and E_1 become comparable. This gives us a value for η_r of about 1.5 to 3×10^6 Pa·s. In the medium load regime, data points were collected with ν_S at 5 μm/s and a_0 of roughly 5 to 10 nm. t_S is equal to 1 to 2 ms. The friction force starts increasing at a temperature of 378 K. This gives us a value for η_r of about 3 to 5×10^6 Pa·s. In the high load regime, data points were collected with ν_S at 5 μm/s and a_0 of roughly 9 to 15 nm. t_S is equal to 1.8 to 3 ms. In this case, the friction force starts increasing at a temperature of 373 K. This gives us a value for η_r of about 6 to 10^6 Pa·s. Similar values for η_r can be obtained from the data by varying the scan velocity at a fixed load shown in Fig. 4.

The increase of contact area and stress at the boundary of incipient sliding is probably sufficient to initiate plastic deformation. This viscoelastic effect is confirmed by the pull-off force dependence on the maximum load (Fig. 5). In that experiment, t_S was higher than in the case of low maximum load: the increase of contact area affects the magnitude of the pull-off force.

The dependence of ν_C on the applied load can be explained using Eq. (7): at fixed speed, the higher the load, the larger the initial contact radius a_0 and the longer t_S. Therefore, ν_C should increase with an increase of the applied load. It is also likely that at T_g, η does not dramatically change from η_g to η_r. Therefore, for a given load, ν_C should also depend on the temperature.

V. CONCLUSIONS

The glass transition of unconfined amorphous polymeric films was investigated using LFM. The goal of this article was to determine if and how the pressure exerted by the tip influences the glass transition. We found that it is not the pressure alone that affects the apparent transition value but also the rate with which the pressure is applied. One important finding is that the shift in the apparent transition temperature from the bulk glass transition temperature is due to the dynamic nature of the experiment and not due to an actual change in the material property, as it would be the case for a hydrostatic compression.

At a fixed scan velocity, the apparent glass transition was found to decrease and to approach the bulk value with increasing load. Similarly, at a fixed load, the apparent glass transition was found to decrease and to approach the bulk value with decreasing scan velocity. These findings might explain the high values reported in the literature for SFM/LFM experiments.

Finally, we discussed our LFM results in terms of critical time scales, which we compared to polymer viscous relaxation times. Our calculations suggest that the viscosity of the polymer films drops to about 10^7 Pa·s at T_g and to about 10^6 Pa·s at 10 K above T_g. Consequently we suggest that the LFM method is a very useful tool to investigate the local and temperature-dependent viscous properties of polymeric films.

ACKNOWLEDGMENTS

The authors thank Miriam Rafailovich and here research group at SUNY Stony Brook. We acknowledge the Shell Faculty Development Program, the NSF MRSEC (DMR96324235), and the Donors of Petroleum Research Fund, administered by the American Chemical Society, for support of this research.

[1] D. Mears, K. Pae, and J. A. Sauer, J. Appl. Phys. **40**, 4229 (1969).
[2] J. R. Stevens, R. W. Coakley, K. W. Chau, and J. L. Hunt, J. Chem. Phys. **84**, 1006 (1985).
[3] P. H. Goldblett and R. S. Porter, J. Appl. Polym. Sci. **9**, 463 (1970).
[4] J. A. Hammerschmidt, B. Moasser, W. L. Gladfelter, G. Haugstad, and R. R. Jones, Macromolecules **29**, 8996 (1996).
[5] R. M. Overney, C. Buenviaje, R. Luginbühl, and F. Dinelli, J. Thermal Anal. Calorimetry **59**, 205 (2000).
[6] R. M. Overney and E. Meyer, MRS Bull. **18**, 26 (1993).
[7] J. A. Hammerschmidt, W. Gladfelter, and G. Haugstad, Macromolecules **32**, 3360 (1999).
[8] C. Buenviaje, S. Ge, M. Rafailovich, J. Sokolov, J. M. Drake, and R. M. Overney, Langmuir **15**, 6446 (1999).

[9] G. H. Gracias, D. Zhang, Y. R. Shen, and G. A. Somorjay, in *Fundamentals of Nanoindentation and Nanotribology*, MRS Symposium Proc. Vol. 522, edited by N. R. Moody, W. W. Gerberich, N. Burnham, and S. P. Baker (Mat. Res. Soc., Warrendale, 1998), pp. 175–180.
[10] R. H. Schmidt, G. Haugstad, and W. L. Gladfelter, Langmuir **15**, 317 (1999).
[11] K. L. Johnson, *Contact Mechanics* (Cambridge University Press, Cambridge, 1985).
[12] *Polymer Handbook*, Vol. X, edited by J. Brandrup and E. H. Immergut (Wiley, New York, 1989).
[13] F. Rodriguez, *Principles of Polymer Systems*, 4th ed. (Taylor & Francis, London, 1996).
[14] R. W. Carpick, N. Agrait, D. F. Ogletree, and M. Salmeron, Langmuir **12**, 3334 (1996).
[15] S. Wu, *Polymer Interface and Adhesion* (Marcel Dekker, New York, 1982).